

Abstract

Duration of intracellular spikes has long been an indicator of pyramidal neurons versus interneurons. Using NEURON and LFPy spike width and amplitude measurements from [Pettersen & Einevoll \(2008\)](#) using the Hay model were replicated. To investigate how spike amplitude and width can classify pyramidal neurons and interneurons, measurements were done in 260 biophysical models from the Blue Brain Project. 1000 electrodes were positioned randomly around each soma to mimic experimental procedures. Probability distributions of the measured widths and amplitudes were compared using AOC curves and a overlap measure. The spike width definitions were found to considerably effect how well classification can be done with the peak-to-peak spike width definition providing the best results. When the spike width combined with spike amplitude significantly increased the separation between interneuron and pyramidal neurons. This suggests that areas in the spike amplitude width space can be attributed to certain kinds of cell types. When a butterworth filter were applied to the spike shapes the separation between interneuron and pyramidal neurons remained showing that classification can still be done using the filtered signals.

Contents

1	Introduction	5
2	Theory	7
2.1	The Neuron	7
2.2	The Cell Membrane	8
2.3	Circuit Model	9
2.4	Action Potential	9
2.5	Multi Compartmental Models	10
2.6	Electrodes	10
2.7	Calculating Extracellular Potential	11
2.8	Neuron & LFPy	12
2.9	Cell Type Classification	13
3	Methods	15
3.1	Spike Width Measurement	15
3.2	Spike Amplitude Measurement	16
3.3	Histogram Similarity Measure	17
3.4	Rotate Cells using PCA	18
3.5	Blue Brain Models	18
3.6	LFPyUtil	18
4	Results	27
4.1	Pettersen & Einevoll (2008) Reproduction	27
4.2	Blue Brain Model Simulations	32
5	Discussion	43
A	Appendix	45
	Bibliography	49

1 | Introduction

Early research showed that interneurons that high firing rates showed "thin" action potentials with short durations. These action potentials could be distinguished from pyramidal cells with longer action potentials and showed a more regular spiking pattern ([Mountcastle et al. \(1969\)](#)). Pyramidal cells exhibiting long and regular spike patterns has since been referred to as regular spiking. These difference between these spike shapes were thoroughly examined in brain slices from rodents.

2 | Theory

2.1	The Neuron	7
2.2	The Cell Membrane	8
2.3	Circuit Model	9
2.4	Action Potential	9
2.5	Multi Compartmental Models	10
2.6	Electrodes	10
2.7	Calculating Extracellular Potential	11
2.8	Neuron & LFPy	12
2.9	Cell Type Classification	13

2.1 The Neuron

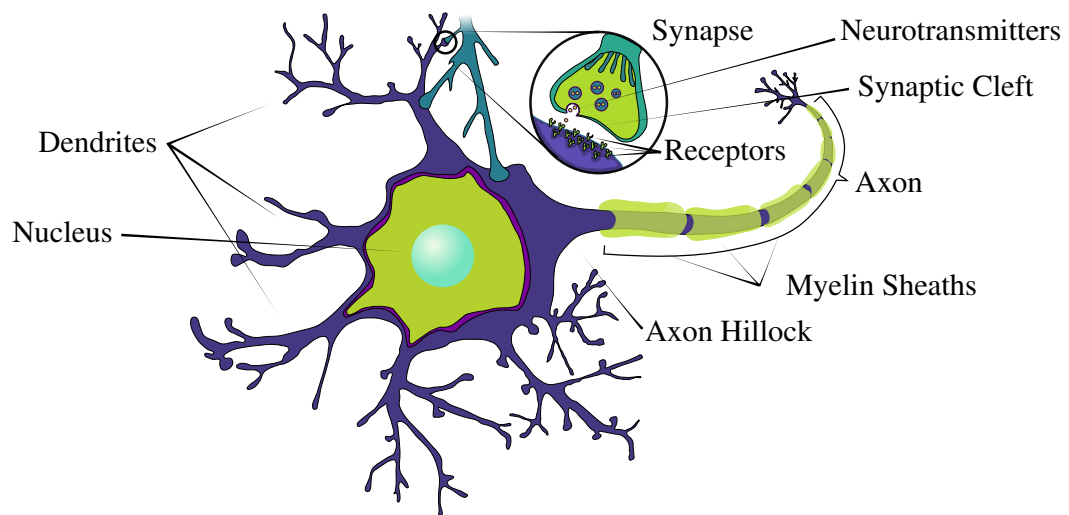


Figure 2.1

Neurons are electrically excitable cells that are a fundamental part of all brain functions. Other names include nerve cells, neurone or more colloquially brain cells. Neurons form in big networks which process information, and in the human brain there is an estimated 10^{11} neurons.

Special proteins in the cell membrane enables the neuron to fire action potentials when it is electrically excited. These action potentials are sharp voltage changes that propagates through the full structure of the neuron. The same properties that makes the neuron able to fire makes the action potential regenerative, meaning it will propagate without decay.

The body of the neuron, the soma, has dendrites and the axon attached to it. The dendrites and the axon are very thin branching structures with a width usually in the order of $1\text{ }\mu\text{m}$. While neurons often have many dendrites directly attached to the soma there is only one axon attached to the soma at the axon hillock. The axon can branch several times before it ends and usually connects to the dendrites of other neurons via synapses.

The synapses are electrically sensitive which allows information to pass between neurons. Though the majority of all synapses are axo-dendritic (axon to dendrite), other junctions are also possible. Other junctions include but are not limited to, dendrite to dendrite, axon to axon and axon to blood vessel. When an action potential reaches a synapse it will activate the synapse and pass information to the connect neuron. The information that is passed along depends on the type of synapse, and if it is of a chemical or electrical type.

2.2 The Cell Membrane

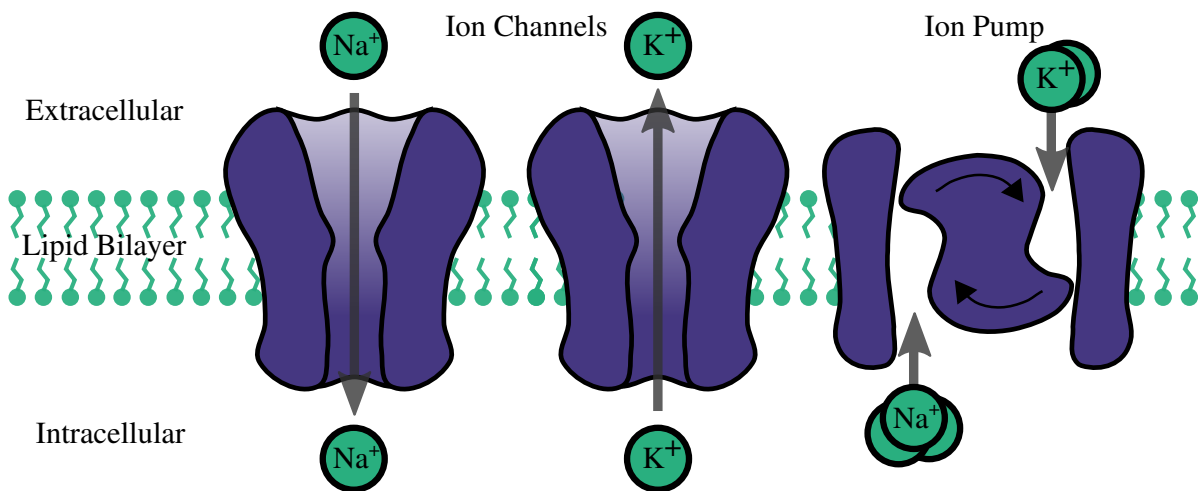


Figure 2.2: Common portrayal of ion channels and pumps in the neuron cell membrane. They are responsible for creating a potential gradient across the membrane. Ion channels have selective permeability of ions. Ion pumps actively transport ions through the membrane, often against the potential gradient. Image modified from [Sterratt et al. \(2011\)](#).

The potential difference between the inside and outside the neurons are caused by different concentrations of ions in the extracellular and intracellular medium. The ions cannot pass through the cell membrane as it consists of a 5 nm lipid bilayer which is mostly impenetrable to ions.

In the membrane sits ion channels and ion pumps which can have selective permeability to ions. Collectively they are referred to as ion transporters. These are created by proteins in complicated shapes. There are over 200 kinds of electrically sensitive ion channels. Together they create a potential gradient across the membrane. The most significant ions in this process are Sodium (Na^+), Potassium (K^+), Calcium (Ca^{2+}), Magnesium (Mg^{2+}) and Chloride (Cl^-). Ion channels are divided between passive channels and active channels where the active channels can change permeability under certain conditions while passive channels have a constant permeability. [Figure 2.2](#) shows a common portrayal of ion channels and pumps.

The ion pumps differ from the channels by actively transporting certain ions through the membrane. For instance, the Sodium-Potassium exchanger pushes two K^+ ions out of the cell for every three Na^+ it pushes into the cell. Doing this creates a net loss of charge inside the cell and the pump is therefore electrogenic. Not all pumps are electrogenic, the Sodium-Hydrogen exchanger transports H^+ and Na^+ without effecting the net charge. For each H^+ ion out of the cell the pump pushes one Na^+ into the cell.

To further understand the electrical activity of neurons it is useful to view the neuron as an electronic circuit where the ion channels, ion pumps and the membrane serve as different electronic components. Figure 2.3 shows the electronic circuit used by Hodgkin and Huxley in their original description of a neuron membrane. Hodgkin & Huxley (1952) and Sterratt et al. (2011)

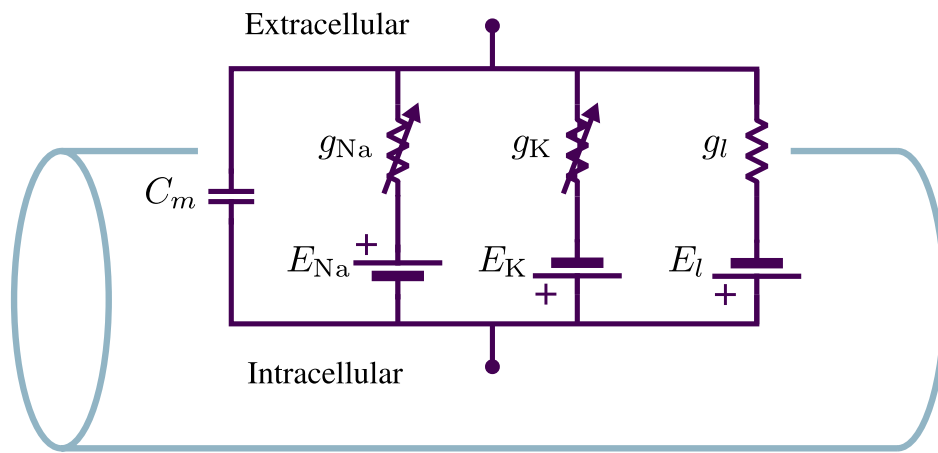


Figure 2.3: Hodgkin and Huxley electrical circuit. Circuit model of a neuron membrane. Each ion channel sets up a potential like a battery with the selective permeability of ions represented by a variable resistor.

2.3 Circuit Model

Hodgkin and Huxley originally tried to understand the electrical properties of neuron by studying squid axons. Given specific functions for the active conductances g_{Na} and g_K , this circuit is enough to describe an important feature of neurons, called action potentials. Alan Hodgkin and Andrew Huxley got the nobel price for their research on the biophysics of action potentials.

The current equation of this neuronal equivalent circuit is

$$I = C_m \frac{dV}{dt} + I_{Na} + I_K + I_l.$$

2.4 Action Potential

Action potentials are sharp increases in the membrane potential followed by a less sharp decrease towards the resting potential. They are generally accepted as the information carriers

between neurons and as such has been a big focus of neuroscience since its discovery.

The shape of the action potentials are directly related to the types and densities of the ion channels present in the membrane. This makes the action potential from neurons to look slightly different, though they all have common features. Figure 2.4 shows the anatomy of an action potential and some common definitions.

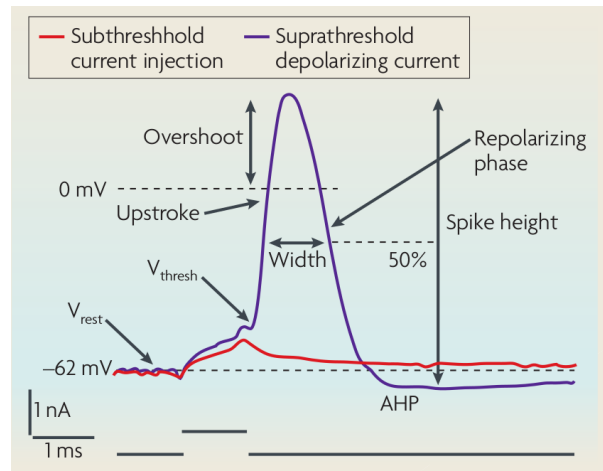


Figure 2.4

In the the depolarization phase the potential rises towards the peak magnitude, while in the repolarization phase the potential decreases towards the cells resting potential. When the potential is below the resting potential it reaches the afterhyperpolarization phase before it returns to its resting potential.

2.5 Multi Compartmental Models

The circuit model represents a patch of a neuronal membrane where the potential across the membrane is the same. If we want to study the voltage change across a longer piece of membrane we want to divide the membrane into parts and have a model for each of them. This is the basis for creating bigger models, where multiple pieces of membrane equivalent circuits are combined into a multi-compartmental model. The size of the compartments are small enough that the membrane potential is considered the same at all places.

2.6 Electrodes

In most cases the membrane potential is wanted when measuring neurons. Though recording the membrane potential is not always feasible, especially in living subjects. Most knowledge about the physiological function of the brain is based on the recordings from single point electrodes.

There are several types of electrodes and are always improving in quality. Earlier studies were often limited by the precision of the instruments. The type of electrodes used depends on several factors. An often used type of electrode are tetrodes consisting of four very small electrodes bundled together. The size of each electrode is generally around 30 μm in diameter.

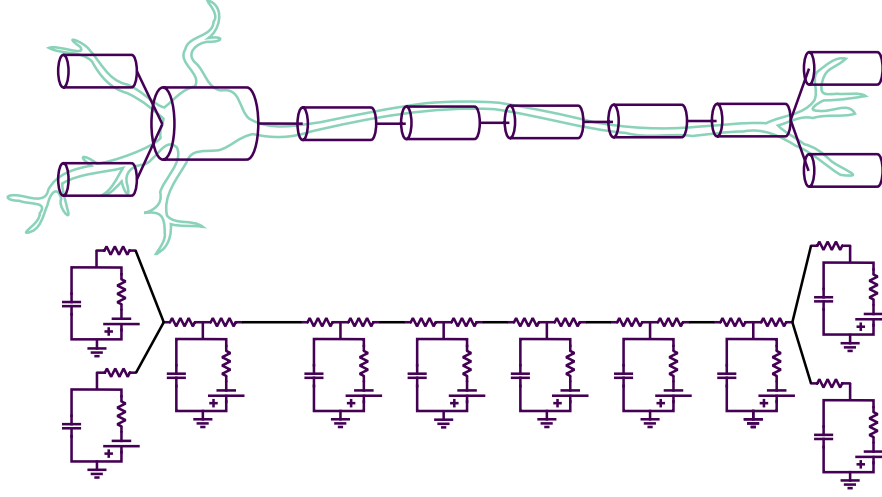


Figure 2.5: Compartmental model.

Raw data from electrodes are usually band pass filtered to remove unwanted noise from the signal. A big source of noise come at low frequencies below about 300 Hz comes from populations of neurons firing. This band of frequencies are sometimes referred to as the local field potential.

2.7 Calculating Extracellular Potential

The extracellular potential is the electric potential generated from the transmembrane currents in the neurons. When a neuron fires this can be seen from the extracellular potential which will have a spike which is similar to the intracellular spike.

By modelling the neuron as compartments and approximating each compartment as a spherical volume current source at position \mathbf{r}_0 , the potential at position \mathbf{r} at time t will be,

$$\mathbf{E}(\mathbf{r}, t) = \frac{1}{4\pi\sigma} \frac{I_0(t)}{|\mathbf{r} - \mathbf{r}_0|} \quad (2.1)$$

$$\mathbf{E}(\mathbf{r}, t) = \sum_{n=1}^N \frac{1}{4\pi\sigma} \frac{I_n(t)}{|\mathbf{r} - \mathbf{r}_0|} \quad (2.2)$$

Potential from compartments modelled as line sources.

$$\mathbf{E}(\mathbf{r}, t) = \frac{1}{4\pi\sigma} \sum_{n=1}^N I_n(t) \frac{dr_n}{|\mathbf{r} - \mathbf{r}_0|} \quad (2.3)$$

$$= \frac{1}{4\pi\sigma} \sum_{n=1}^N I_n(t) \frac{1}{\Delta s_n} \log \left| \frac{\sqrt{h_n^2 + \rho_n^2} - h_n}{\sqrt{l_n^2 + \rho_n^2} - l_n} \right| \quad (2.4)$$

Taken from [Lindén et al. \(2013\)](#)

This equation rests on two assumptions,

1. The permeability μ of the extracellular medium is the same as that of vacuum μ_0 .
2. The quasistatic approximation which lets the time derivatives, $\partial E/\partial t$, be ignored as source terms. See ??

The extracellular potential can be calculated using Maxwell's equations and the continuity equation if the spatial distribution (morphology) of transmembrane currents and the extracellular conductivity is known.

In the quasistatic approximation, since $\nabla \times \mathbf{E} = 0$, the electric field can be expressed with a scalar potential.

Forward problem = calculate the potential from the current source, inverse problem is used in magnetoencephalography (important). The amplitude of a spike in the extracellular potential is usually in the magnitude of $< 200\mu\text{V}$. The noise of electrodes vary, but can be as much as $20\mu\text{V}$. This limits the range electrodes can record from.

The currents sum to zero, while the spike is very visible, there are many small currents in the dendrites with opposite current. (Hämäläinen et al. 1993)

The extracellular spike width tend to increase with distance from soma because of the neuronal morphology. This article used a passive neuron model with different morphologies to show that the spike width increases with distance to soma. The spike amplitude also decreases with distance to soma and seems to follow a power law. (Pettersen & Einevoll 2008).

The shape of extracellular spikes are mainly dependent on the membrane currents and the morphology of the cell. Some of the effects from the morphology of the cell are increased spike width and decreased amplitude from distance to soma.

Recording is usually done using electrodes, this makes recording the membrane potential more challenging than recording from the extracellular medium as the electrode has to be very close or inside the cell. At the time of writing, recording the membrane potential of a conscious subject is nearly impossible, this makes understanding extracellular potentials vital for current research.

Early calculations was done by Rall 1962 investigating the interaction between action potentials and synapses using cylinders as the current source. (TODO: Read article, make more understandable.) Holt and Koch 1999 added compartmental models to reconstruct pyramidal neurons.

The information about the transmembrane current is usually difficult to obtain, as well as the morphology.

2.8 Neuron & LFPy

LFPy is a Python module that uses Neuron and the mentioned methods to calculate the electric field outside the neuron. Lindén et al. 2013

Background

2.9 Cell Type Classification

The shape of action potentials is a big focus of this project as they are a direct product of the types and densities of the ion channels present in neurons. This is again based on the genetical makeup of the neurons. This makes the action potential a candidate for a classification parameter of different types of neurons.

It was early observed that the shape of action potentials are different for individual neurons. Mountcastle et al. (1969) discovered what they called regular spiking and fast spiking.

Mountcastle et al. 1969. Results are based on spike width and amplitude. The basis for all spike shapes are the types and concentrations of ion channels. This is the central factor that decides if the neuron has short or long action potentials. A number things has been observed that can change spike spike width. Factors that change action potentials width: * Firing frequency. * Input current. Higher current gives higher frequency. * Number of previous spikes. * Bursting behavior. * Backpropagating action potentials.

3 | Methods

Methods mentioned here have been developed specifically for this research.

3.1	Spike Width Measurement	15
3.2	Spike Amplitude Measurement	16
3.3	Histogram Similarity Measure	17
3.4	Rotate Cells using PCA	18
3.5	Blue Brain Models	18
3.6	LFPyUtil	18
3.6.1	About	18
3.6.2	Minimal Working Examples	19
3.6.3	List of Simulation Classes	25

3.1 Spike Width Measurement

There are several definitions of spike width used in neuroscience. In some cases the definition of the spike width is not mentioned and simply addressed as the spike duration. The most commonly used spike width definition is the spike width at half amplitude ([Bean \(2007\)](#)).

Often the choice of spike width definition is chosen by seeing which gives the best bimodal distribution. Of some spike width definitions encountered in the literature were: width at half amplitude, peak-to-peak width, width at base and width of afterhyperpolarization phase.

Most extracellular spikes have a minimum value greater than the maximum value, but this is not always the case at certain positions of the neuron.

Peak-to-peak Width: Referred to as type I spike width in the code. The width is measured as the time from the minimum potential to the maximum. This is a rough measure of the time from the polarization phase to the afterhyperpolarization phase.

The definition can be implemented by measuring the width from minimum to maximum value, but in cases where the spike is flipped the definition must also change. As such the implementation was done by defining the positive axis along the maximum absolute value and calculate the time from the maximum value to the preceding minimum value.

Half Amplitude Width: Width is measured as the duration the spike is below half amplitude of the signal measured from the baseline. The baseline is commonly set as the value of the start of the signal, though this is not always well defined. In many cases the start of the signal is chosen trivially and if exciting a neuron with a square current the membrane potential will rise

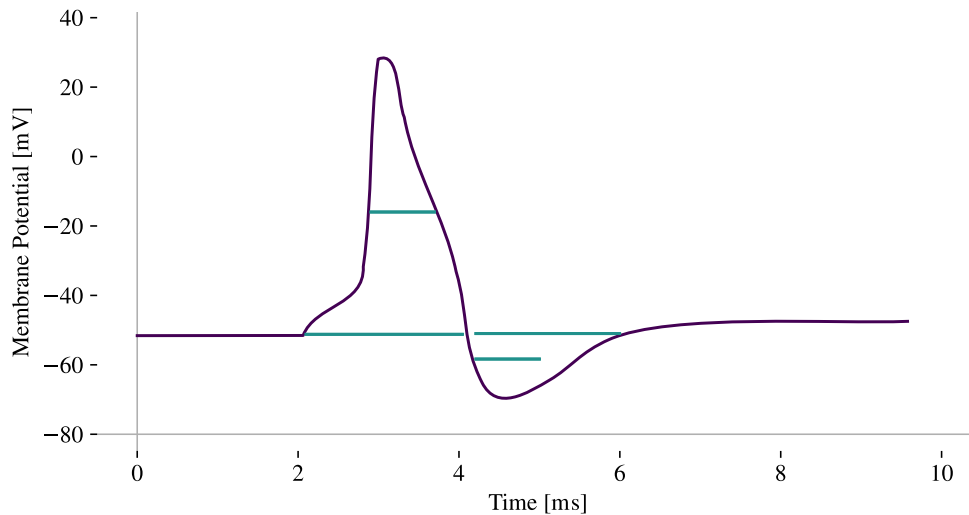


Figure 3.1

gradually. A more accurate description would be to set the baseline at the firing threshold of the intracellular spike. This is not possible in the case of extracellular spikes, but here the baseline can simply be set as 0.

Width at Base: Experimentally the width at the baseline is commonly used. It can be difficult to get a good resolution as spikes are very short and measured width at baseline gives a longer duration than width at half amplitude.

Calculating width at baseline can pose problems when doing computer simulations of extracellular spikes as there is no firing threshold. If the baseline is set at 0 the duration of spike has a tendency to become unnaturally long due to the slight potential created by the charging of the membrane before firing. Experimentally this is not a problem as there is always noise in the signal. When attempting to measure the width at baseline for extracellular simulations the baseline can either be set to some fraction of max amplitude or set as a constant value. Both of these solutions have drawbacks however because it makes the threshold be chosen trivially.

Width of afterhyperpolarization: Certain features of an action potential can be connected to the activation of some ion channels. That is why in some cases the duration of the afterhyperpolarization is desired. Two ways to define this duration is the width at base or width at half amplitude.

3.2 Spike Amplitude Measurement

Amplitude is easier to calculate than the width of a spike, but there are still different ways to define the amplitude. In most cases the amplitude is defined as the distance from a baseline, in a similar manner as a sinusoid.

3.3 Histogram Similarity Measure

To assess width and amplitude definitions on how well they classify interneuron from pyramidal neurons one needs a way to analyze the resulting data. To assess how well a variable can be separated into groups, such as the width from either pyramidal neurons or interneurons, is a classification problem. Classification is a big field and a high quality classification algorithm is beyond the scope of this project. If the separation between two variables are clear and bimodal there should still be possible to declare that this variable can be used as a classification parameter.

If we assume electrodes are placed randomly around a neuron and calculate the amplitude and width one can create a probability distribution of that measure. This is done by creating a histogram of the samples where the height of the bars are equal to the number of samples within that bin. By normalizing this distribution we get the measured probability distribution of that variable.

Comparing histograms is of fundamental importance in pattern classification, clustering and information retrieval problems. From this field we can borrow a measure of the difference between histograms. This measure is frequently referred to as the histogram distance. As histograms can be viewed as points in multidimensional space the histogram distance are also commonly referred to as a metric.

Choosing an appropriate metric should be fit to the specific data and results desired. To keep things simple two metrics have been chosen for this project, the (ROC AUC) and a simple intersection metric.

Receiver Operator Characteristic Area under Curve Useful binary classifier.

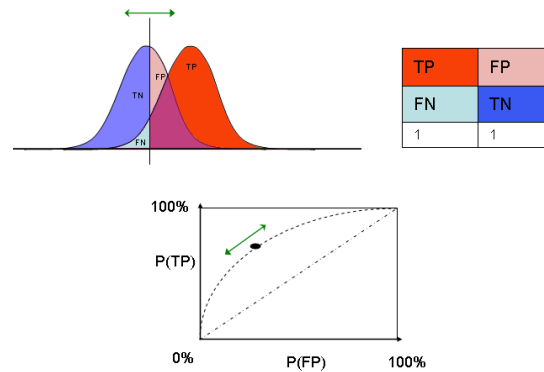


Figure 3.2: ROC curve.

Simple Overlap The metric is simply defined as the overlap of two histograms. It can be defined similar to the intersection divided by the union of sets, the Jaccard Index. One source named this metric the histogram jaccard metric.

This metric was chosen because ROCAUC is only defined for one dimensional data and because of its simplicity. The metric measures 0 when the two variables share no data in com-

mon and 1 if compared to itself.

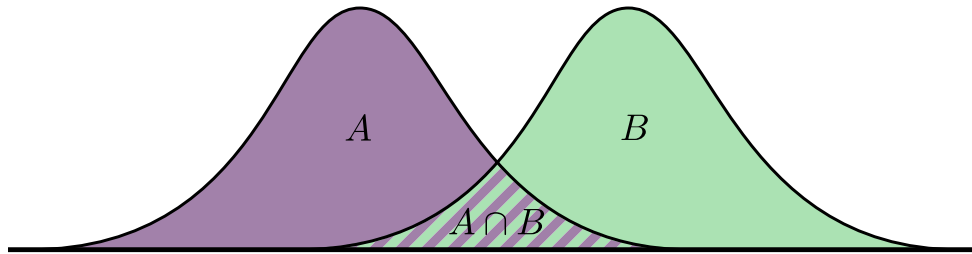


Figure 3.3: An intersection metric as a way to measure the similarity between two distributions.

3.4 Rotate Cells using PCA

3.5 Blue Brain Models

Obtaining a reconstruction of the morphology of neurons is an arduous task which has limited the number of fully reconstructed neuron models.

The Human Brain Project Neocortical Microcircuit Collaboration Portal (bbp.epfl.ch/nmc-portal/welcome, [Ramaswamy et al. \(2015\)](#)) released multiple neuron models from the hind limb somatosensory cortex of 2-week-old Wistar Han rats. The models have been classified into both morphological and electrophysical types with full morphological reconstruction.

The neuron models are based on the classification criteria set by the Blue Brain team.

3.6 LFPyUtil

3.6.1 About

LFPyUtil is a python package that was created for this project with the purpose to simplify the simulation pipeline for multiple neurons and creating an easy to use interface when developing new simulations. LFPyUtil extends and uses the package LFPy to accomplish this. Simulations can be run in parallel and data from simulations can automatically be saved and loaded to avoid unnecessary processing time. LFPyUtil has 9000 lines of code, documentation can be found at www.documentation.lastis.com.

LFPy is a Python package created to calculate extracellular potentials. Another major feature is wrapping the cell model and electrodes from the NEURON simulation environment into

Python objects, such as the `LFPy.Cell` and `LFPy.StimIntElectrode` classes. This makes working with NEURON more pythonic as it can be argued that NEURON is state-based. That is, even though the Python interface of NEURON uses objects, the objects are bound to the state system. In practical terms this means that all functions and variables with NEURON are global static.

While NEURON has support for parallel processing of single simulations it does not have any inherent support for running multiple independent simulations. For "embarrassingly parallel" situations like this, users have had to resort to creating their own methods to start each simulation independently. For instance, one solution would be to use a Python script to run other scripts through the command line, effectively starting new processes. In addition there is no function to reset the simulation environment which can make previous simulations affect later ones.

LFPyUtil uses Python's multiprocessing package to run independent simulations and thus overcomes some of the shortcomings of NEURON and LFPy.

3.6.2 Minimal Working Examples

These examples show how to create a new custom simulation from scratch and how to use them with LFPyUtil. A basic understanding of object-oriented programming and Python is required.

To run a simulation LFPyUtil must first have a `LFPy.Cell` object it can use to interact with the model. The cell object gives access to functions such as `Cell.simulate()` which starts the NEURON simulation. A template of such a function can be seen in [listing 1](#). A fully working example of such a function can be seen in the appendix (??).

Listing 1: `load_model_simple.py`

```
1 import LFPy
2
3 def get_cell(neuron_name):
4     """
5     Load a specific model based on the input string and return
6     a LFPy Cell object
7
8     :param string neuron_name:
9         String to identify the neuron model that will be loaded.
10    :returns:
11        Cell object from LFPy.
12    """
13
14    cell = LFPy.Cell( some cell parameters ... )
15    return cell
16
```

LFPyUtil use subclasses of the class `LFPyUtil.sims.Simulation`. to organize simulations. [Listing 2](#) shows a very minimal example of such a subclass. If the functions `simulate`, `process_data` and `plot` are not overridden, a `NotImplementedError` will be raised.

Listing 2: new_simulation_class_simple.py

```
1 from LFPy_util.sims import Simulation
2
3 class CustomSimulation(Simulation):
4     def __init__(self):
5         # Inherit the LFPyUtil simulation class.
6         Simulation.__init__(self)
7         # These values are used by the super class to save and load data.
8         self.set_name("custom_sim")
9
10    def simulate(self, cell):
11        pass
12
13    def process_data(self):
14        pass
15
16    def plot(self, dir_plot):
17        pass
```

The LFPyUtil simulation class has been created to reflect four parts of a typical neuron simulation. (1) Initialization, (2) simulation/gather data, (3) processing data and (4) plotting the data. These four parts are retained in the initialization of the object, the `__init__()` function, a simulation function `simulate(cell)`, a process function `process_data()` and a plotting function `plot()`. Run parameters, plot parameters and data are stored in dictionaries in the simulation class and the variables are named `run_param`, `plot_param` and `data` respectively. The LFPyUtil simulation class has additional properties that among other things enable saving and loading data and naming those files. Because of this a new simulation class should inherit LFPyUtil's simulation class.

Listing 3 defines a simulation class that inherits the LFPyUtil simulation class, but adds some more functionality. The function `simulate` inserts a stimulus electrode and applies a current to soma with parameters defined in `__init__`. The membrane potential is then stored in the data dictionary. The function `process_data` creates a normalized version of the membrane potential and saves it. The function `plot` plots the membrane potential. To exemplify the use of `plot_param`, a conditional statement is used to decide whether or not to plot the normalized version.

Listing 3: new_simulation_class.py

```

1 import LFPy
2 import LFPy_util
3 import matplotlib.pyplot as plt
4 from LFPy_util.sims import Simulation
5
6 class CustomSimulation(Simulation):
7     def __init__(self):
8         """
9         Typical initialization function, called when a new instance
10         is created.
11         """
12         # Inherit the LFPyUtil simulation class.
13         Simulation.__init__(self)
14         # These values are used by the super class to save and load data.
15         self.set_name("custom_sim")
16
17         # Create some parameters that are used by the simulate method.
18         self.run_param['delay'] = 100 # ms.
19         self.run_param['duration'] = 300 # ms.
20         self.run_param['amp'] = 1.0 # nA.
21
22         # Create a parameters used by the plotting function.
23         self.plot_param['plot_norm'] = True
24
25     def simulate(self, cell):
26         """
27         Setup and starts a simulation, then gathers data.
28         """
29         :param LFPy.Cell cell:
30             Cell object from LFPy.
31         """
32         # Create an electrode with LFPy.
33         soma_clamp_params = {
34             'idx': cell.somaidx,
35             'amp': self.run_param['amp'],
36             'dur': self.run_param['duration'],
37             'delay': self.run_param['delay'],
38             'pptype': 'IClamp'
39         }
40         stim = LFPy.StimIntElectrode(cell, **soma_clamp_params)
41         cell.simulate()
42
43         # Store the data.
44         self.data['soma_v'] = cell.somav
45         self.data['soma_t'] = cell.tvec
46
47     def process_data(self):
48         """
49         Process data from the simulate function, usually to prepare
50         the data for plotting. This function creates a normalized
51         version of the membrane potential.
52         """
53         soma_v_norm = self.data['soma_v'].copy()
54         soma_v_norm -= soma_v_norm[0]
55         soma_v_norm /= soma_v_norm.max()
56         self.data['soma_v_norm'] = soma_v_norm
57
58     def plot(self, dir_plot):
59         """
60         Plot data from the simulate and process_data function.
61         This functions plots the membrane potential and the
62         normalized version.
63         """
64         :param string dir_plot:
65             Path to the directory where plots should be saved.
66         """
67         plt.plot(self.data['soma_t'], self.data['soma_v'])
68         # Save the plot to input directory with the name "custom_sim_mem".
69         LFPy_util.plot.save_plt(plt, "custom_sim_mem", dir_plot)
70         # plot_param can be used to affect the plotting.
71         if self.plot_param['plot_norm']:
72             plt.plot(self.data['soma_t'], self.data['soma_v_norm'])
73             # Save the plot to input directory.
74             LFPy_util.plot.save_plt(plt, "custom_sim_mem_norm", dir_plot)
75

```

The newly created simulation class can now be used to run a complete simulation as seen in [listing 4](#).

Listing 4: first_simulation.py

```
1 # Import the get_cell function defined previously.
2 from load_model import get_cell
3
4 # Import the newly defined simulation class.
5 from new_simulation_class import CustomSimulation
6
7 # Load the model, using a string to identify which model will be returned.
8 cell = get_cell("pyramidal_1")
9
10 # Create an instance of the custom simulation class.
11 sim_custom = CustomSimulation()
12
13 sim_custom.simulate(cell)
14 sim_custom.process_data()
15 # Plots are stored in a folder called first_simulation.
16 sim_custom.plot("first_simulation")
```

If one attempted to run the simulation function in [listing 3](#) more than once in the same program, we would experience that subsequent simulations would be affected by previous simulations. This is because a new electrode will be applied once for each call to the simulation function. With NEURON or LFPy there are no easy way to reset the environment to prevent this. One workaround is to use Python's multiprocessing package to create multiple independent processes. Doing this for every simulation will require excessive amounts of code. LFPyUtil can simplify this with tools that requires less code and are compatible with classes like the one defined in [listing 3](#).

The class `LFPyUtil.Simulator` accepts one or more objects that inherit LFPyUtil's simulation class and can run them either in serial or parallel and either in a new independent processes or in the same process. [Listing 5](#) shows how the newly created simulation class can be used with `LFPyUtil.Simulator` to run multiple simulations in parallel and in independent processes.

Listing 5: multiple_simulations.py

```
1 import LFPy_util
2 from load_model import get_cell
3 from new_simulation_class import CustomSimulation
4
5 sim = LFPy_util.Simulator()
6 sim.set_cell_load_func(get_cell)
7 # The string is passed to the get_cell function.
8 sim.set_neuron_name("pyramidal_1")
9
10 sim_custom_1 = CustomSimulation()
11 sim_custom_1.run_param['amp'] = 1.25 # nA
12
13 sim_custom_2 = CustomSimulation()
14 sim_custom_2.run_param['amp'] = 0.75 # nA
15 # Avoid sim_custom_2 overwriting the data from sim_custom_1.
16 sim_custom_2.set_name("custom_sim_2")
17
18 # Add the simulations to a list we want to run.
19 sim.push(sim_custom_1)
20 sim.push(sim_custom_2)
21
22 sim.simulate()
23 sim.plot()
```

The function `Simulator.push` adds the simulation objects to a list. When the function `Simulator.simulate()` is ran, the `simulate()` function of those objects will be

called in parallel and in independent processes. The `Simulator.plot()` function will call `process_data()` and `plot(dir_plot)` functions of those objects, and the parameter `dir_plot` will be created based on the name of the simulation class and the name of the neuron name. In this case the plots are stored in the directories `./pyramidal_1/plot/custom_sim/` and `./pyramidal_1/plot/custom_sim_2/`.

The `Simulator` class utilizes save and load features of the simulation class when the `Simulator.simulate()` function is called. This makes the dictionaries `data` and `run_param` be saved to file. If `Simulator.plot()` is ran without `Simulator.simulate()` being called first, the program will notice that the simulations are missing the `data` dictionary. It will then attempt to load the `data` and `run_param` from file. After [listing 5](#) has been run once line 22 can thus be commented out and the data will be loaded instead of running the simulation.

LFPyUtil comes with some predefined simulations that have been used for results in this article. [Listing 6](#) shows an example of how to use the predefined simulations.

[Listing 6](#): predefined_simulations.py

```
1 import LFPy_util
2 from load_model import get_cell
3
4 sim = LFPy_util.Simulator()
5 sim.set_cell_load_func(get_cell)
6 sim.set_output_dir("predefined_simulations")
7
8 sim.set_neuron_name("pyramidal_1")
9
10 sim_electrode = LFPy_util.sims.MultiSpike()
11 sim_electrode.run_param['spikes'] = 3
12
13 sim_intra = LFPy_util.sims.Intracellular()
14
15 # Add the simulations to a list we want to run.
16 sim.push(sim_electrode, False)
17 sim.push(sim_intra)
18
19 sim.simulate()
20 sim.plot()
```

The class `MultiSpike` searches for the input current that will result in 3 spikes and then applies that electrode. It also plots some figures, like the input current and the spikes. `Intracellular` simulates and plots statistics about some intracellular recordings. The details of the predefined simulations can be found in [section 3.6.3 List of Simulation Classes](#).

Note the extra condition, `False`, in line 16. This tells the simulator that this simulation should not be run in an independent process. When the `MultiSpike` simulation is finished, the electrode it used to generate 3 spikes is still loaded in NEURON. When the simulation function of `Intracellular` runs, the electrode will excite the neuron and generate 3 spikes. This feature can be used to link simulations and makes the simulations modular.

The previous examples use only one neuron model. To be able to run many different models it is useful to define a function such as the one in [listing 7](#).

Listing 7: simulator.py

```
1 import LFPy_util
2 from load_model import get_cell
3
4 def get_simulator(neuron_name):
5     sim = LFPy_util.Simulator()
6     sim.set_cell_load_func(get_cell)
7     sim.set_output_dir("multiple_neurons")
8     sim.set_neuron_name(neuron_name)
9
10    sim_electrode = LFPy_util.sims.MultiSpike()
11    sim_electrode.run_param['spikes'] = 3
12
13    sim_intra = LFPy_util.sims.Intracellular()
14
15    sim.push(sim_electrode, False)
16    sim.push(sim_intra)
17
18    return sim
```

To do the same simulation as in [listing 6](#), one could write:

Listing 8: run_simulator.py

```
1 from simulator import get_simulator
2
3 sim = get_simulator("pyramidal_1")
4 sim.simulate()
5 sim.plot()
```

[Listing 9](#) runs the two predefined simulations with two different neuron models. The class `LFPyUtil.SimulatorManager` takes a list of neuron names and passes them to the `get_simulator(neuron_name)` function in [listing 7](#). The parameter `neuron_name` are the elements of the list of neuron names. After running the code once, `sim.simulate()` can be commented out and the simulations will load data instead of running the simulations.

The final simulation uses three files: [listing 1](#), [listing 7](#) and [listing 9](#) and 2 predefined simulation classes.

Listing 9: multiple_neurons.py

```
1 from simulator import get_simulator
2
3 neurons = ["pyramidal_1", "pyramidal_2"]
4
5 simm = LFPy_util.SimulatorManager()
6 # Number of LFPy_util.Simulator objects that will run in parallel.
7 simm.concurrent_neurons = 8
8 simm.set_neuron_names(neurons)
9 simm.set_sim_load_func(get_simulator)
10
11 simm.simulate()
12 simm.plot()
```


3.6.3 List of Simulation Classes

These are the predefined simulation classes included in LFPyutil. Each class has a simulation function that sets up electrodes and/or recording positions. Here the function and implementation of each class is explained.

SphereRand: SphereRand places electrodes placed in uniformly distributed locations around the soma within a default radius of 50 μm . Spike timing is detected by thresholding the soma membrane potential. That timing is applied to all electrodes such that all electrodes measure the same part of the simulation. If the signal has several spikes the spike index must be supplied, the default setting uses the first spike.

SphereRand Parameters:

Listing 10: SphereRand Parameters

```
1 class SphereRand(Simulation):
2     def __init__(self):
3         Simulation.__init__(self)
4         # Used by the super save and load function.
5         self.set_name("sphere")
6
7         self.debug = False
8         self.run_param['N'] = 1000
9         self.run_param['R'] = 50
10        self.run_param['sigma'] = 0.3
11        self.run_param['ext_method'] = 'som_as_point'
12        self.run_param['seed'] = 1234
13
14        self.process_param['amp_option'] = 'both'
15        self.process_param['pre_dur'] = 16.7 * 0.5
16        self.process_param['post_dur'] = 16.7 * 0.5
17        self.process_param['threshold'] = 3
18        self.process_param['width_half_thresh'] = 0.5
19        self.process_param['bins'] = 11
20        self.process_param['spike_to_measure'] = 0
21        self.process_param['assert_width'] = False
22        self.process_param['assert_width_I_low'] = 0.2 # ms
23        self.process_param['assert_width_I_high'] = 3 # ms
24        self.process_param['assert_width_II_low'] = 0.1 # ms
25        self.process_param['assert_width_II_high'] = 2.0 # ms
```


4 | Results

4.1	Pettersen & Einevoll (2008) Reproduction	27
4.1.1	Setup	27
4.1.2	Results	30
4.2	Blue Brain Model Simulations	32
4.2.1	Choosing the Optimal Width Definition	33
4.2.2	Choosing the Optimal Amplitude Definition	36
4.2.3	Combining Spike Width and Amplitude	37
4.2.4	Subclasses	37
4.2.5	Filtering effects	38
4.2.6	Comparing Results	39

4.1 Pettersen & Einevoll (2008) Reproduction

To verify that the simulation environment could be trusted some results from [Pettersen & Einevoll \(2008\)](#) was replicated. Specifically the spike width and amplitude dependency in relation to the distance from soma was compared to current results.

4.1.1 Setup

Model: The [Mainen & Sejnowski \(1996\)](#) morphology was used with a passive model, which is the same model used in [Pettersen & Einevoll \(2008\)](#). The cell was rotated using PCA (principal component analysis) on the compartment positions. This calculates three orthogonal vectors such that the positions of the compartments has the greatest variance along the first principal component, second highest along the second and third most along the third. The first principal component

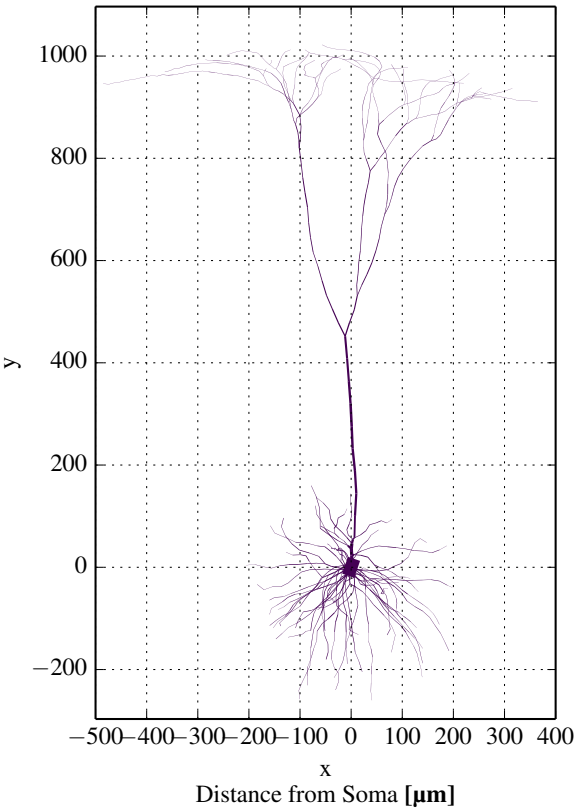


Figure 4.1: Morphology of [Mainen & Sejnowski \(1996\)](#) cell. The apical dendrites are located along the y-axis after rotation with PCA.

was made parallel to the y-axis which puts the apical dendrites along this axis (fig. 4.1).

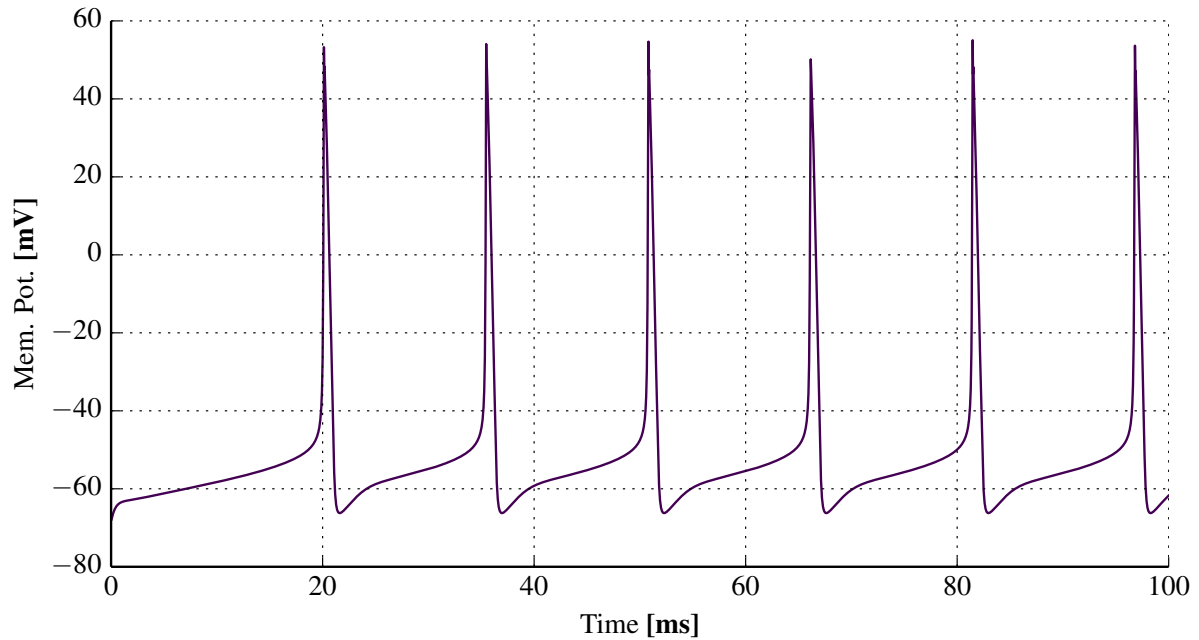


Figure 4.2: Simulation of the Connor-Stevens model using parameters from Dayan & Abbott (2001). A similar graph is shown in fig. 6.1 (B) in their book.

Spike Generation: To recreate the action potential used in Pettersen & Einevoll (2008) a spike was generated using the Connor-Stevens model (Connor & Stevens (1971) and Connor, Walter, et al. (1977)) using the same parameters as Dayan & Abbott (2001) and Pettersen & Einevoll (2008). In fig. 4.2 the Connor-Stevens simulation is shown where the second spike was used for further analysis. This spike had an amplitude of 119.49 mV from baseline. The baseline was estimated to -53.26 mV and the peak at 53.26 mV. These values matches Dayan & Abbott (2001), but not the spike used in Pettersen & Einevoll (2008) which had an amplitude of 83 mV from baseline. Pettersen & Einevoll (2008) does not go into further detail about the creation of the action potential other than stating the action potential were similar to Dayan & Abbott (2001). The difference might be explained by the fact that action potentials from pyramidal neurons often peaks at 20 mV, and that this was achieved by scaling the original signal from the Connor-Stevens model. To compensate for the difference the action potential used in further simulations were scaled to 83 mV (fig. 4.3).

The input current was set to $12.6 \mu\text{A cm}^{-2}$, and was very carefully adjusted to make the magnitude spectrum (fig. 4.5) similar to Pettersen & Einevoll (2008) figure 3. Without adjustment the magnitude spectrum tended to have a different initial value, from 6 to 8 mV, and was not as smooth.

Parameters: Parameters for the Neuron simulation were the same as Pettersen & Einevoll (2008) and the aforementioned action potential was used as a boundary condition in soma. This

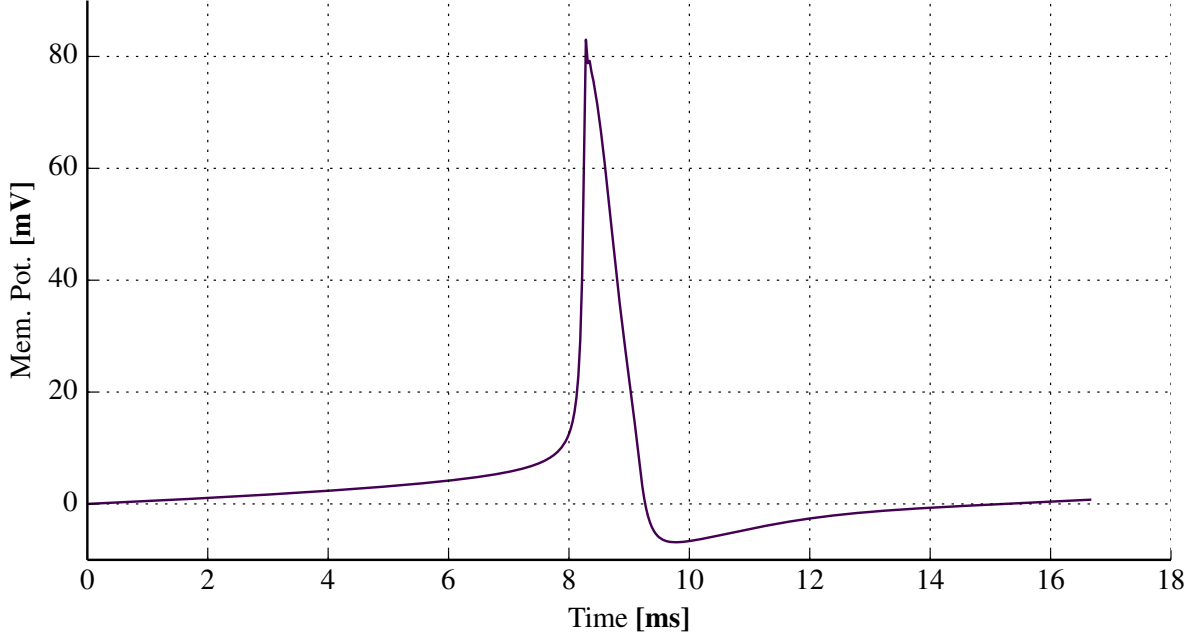


Figure 4.3: The second spike in fig. 4.2 scaled to 83 mV to match the action potential used in Pettersen & Einevoll (2008).

was accomplished by setting the membrane potential equal to the action potential in all soma sections using the `.play` vector function in Neuron. This "excites" the neuron even though there are no ion channels in the model.

Membrane resistance $R_m = 30 \text{ k}\Omega \text{ cm}^{-2}$, membrane capacitance $C_m = 1 \text{ }\mu\text{F cm}^{-2}$, axial resistance $R_a = 150 \text{ }\Omega \text{ cm}^{-2}$, time resolution $dt = 2^{-5} \text{ ms}$. The reversal potential was set to zero.

Electrode Positions: Recording sites were placed in the xz -plane at 11 linearly spaced positions along 36 lines with equal angular spacing (fig. 4.4). Pettersen & Einevoll (2008) states the recording positions were in the plane perpendicular to the apical dendrites, this is ensured by the rotation done with PCA and putting the electrodes in the xz -plane.

Spike Width & Amplitude: A baseline was set as the value at the start of the signal. Amplitude was calculated as the difference between the maximum value and the baseline. The spike width was calculated as the width at half maximum value.

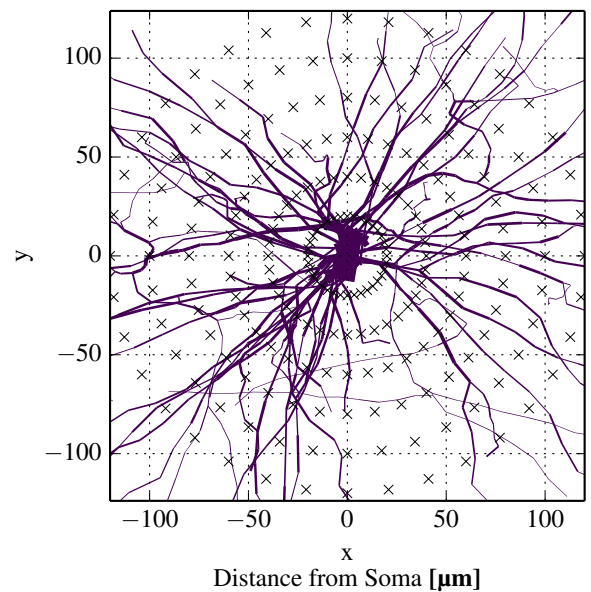
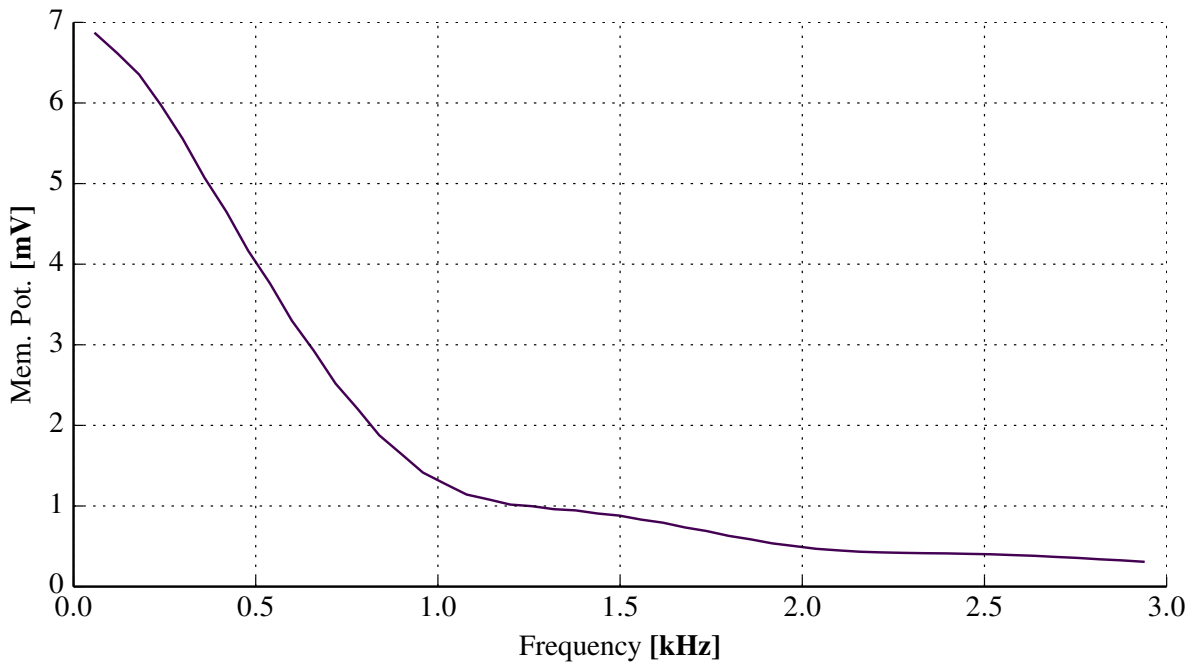


Figure 4.4: Electrode positions placed in a plane around soma perpendicular to the axis along the apical dendrites.

At $dt = 2^{-5}$ ms, the spike width from the Connor-Steven model was 0.5625 mV. This is similar to the reported spike width from [Pettersen & Einevoll \(2008\)](#) which was 0.55 ms. Because the dt used in their simulations was $dt = 2^{-5}$ ms = 0.031 25 ms, their resulting spike width must have been rounded to the nearest 0.05 ms.

4.1.2 Results

The action potential that was used in [Pettersen & Einevoll \(2008\)](#) is similar to the one used here. The amplitude of the fourier transform is displayed in [fig. 4.5](#), which is in close resemblance to the action potential in [fig. 3](#) in the paper.



[Figure 4.5](#): Magnitude specter of simulated somatic membrane potential.

The spike width increases with the distance from soma as seen in [fig. 4.6](#). These results from [Pettersen & Einevoll \(2008\)](#) show an initial spike width of about 0.5 ms at 20 μ m to 0.8 ms at 120 μ m. Current results are higher than the reported widths by about 0.1 ms at every distance. The spike width is defined as width of the negative phase at 25% of the maximum amplitude. If the spike width is adjusted to 35% of the maximum amplitude the results match nearly perfectly, though the importance of this is unclear.

Sudden changes in spike width was experienced with increased distance from soma. Above 200 μ V the most of the spikes shapes are not well defined. This was also reported in [Pettersen & Einevoll \(2008\)](#).

[Figure 4.7](#) shows the spike amplitude with logarithmic axes. The exact results from [Pettersen & Einevoll \(2008\)](#) are not available but the approximate value can be seen from their plots and the exponential decay $1/r^n$ was reported as $n \sim 2$ at 20 μ m and $n \sim 2.5$ at 120 μ m. Current results are not identical to those findings and have an exponent of $n = 2$ at 20 μ m

and $n = 2.8$ at $120\ \mu\text{m}$. The value of the amplitude was about $350\ \mu\text{V}$ in [Pettersen & Einevoll \(2008\)](#), but the current model only gives an amplitude of $120\ \mu\text{V}$ at $20\ \mu\text{m}$.

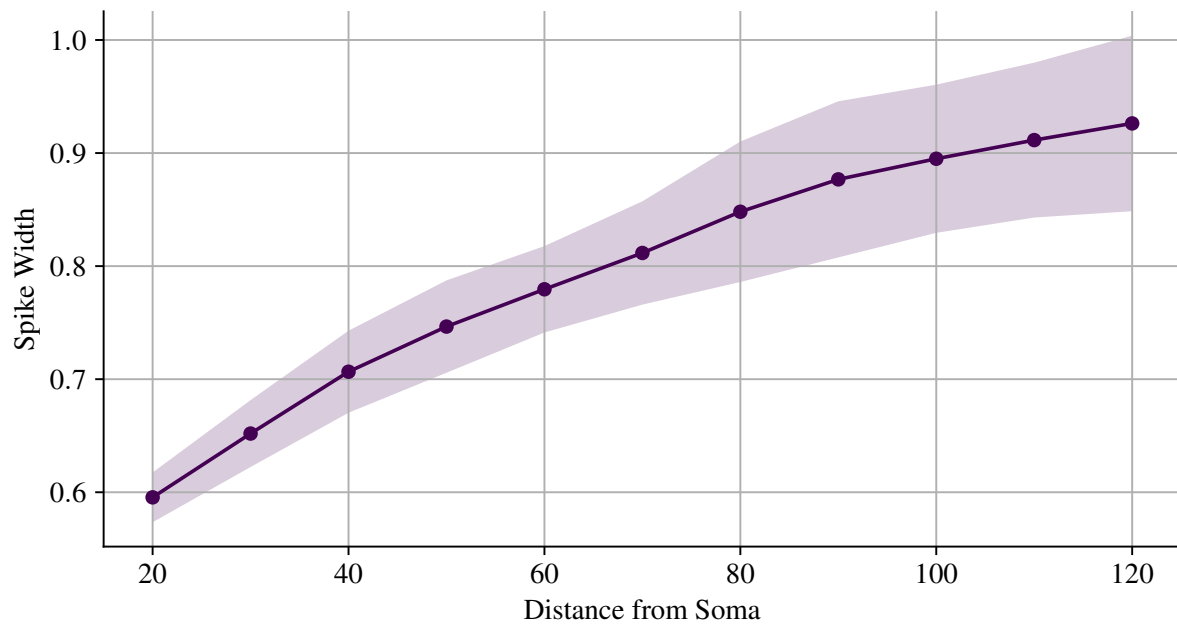


Figure 4.6: Spike width over distance. Mean \pm 1 std.

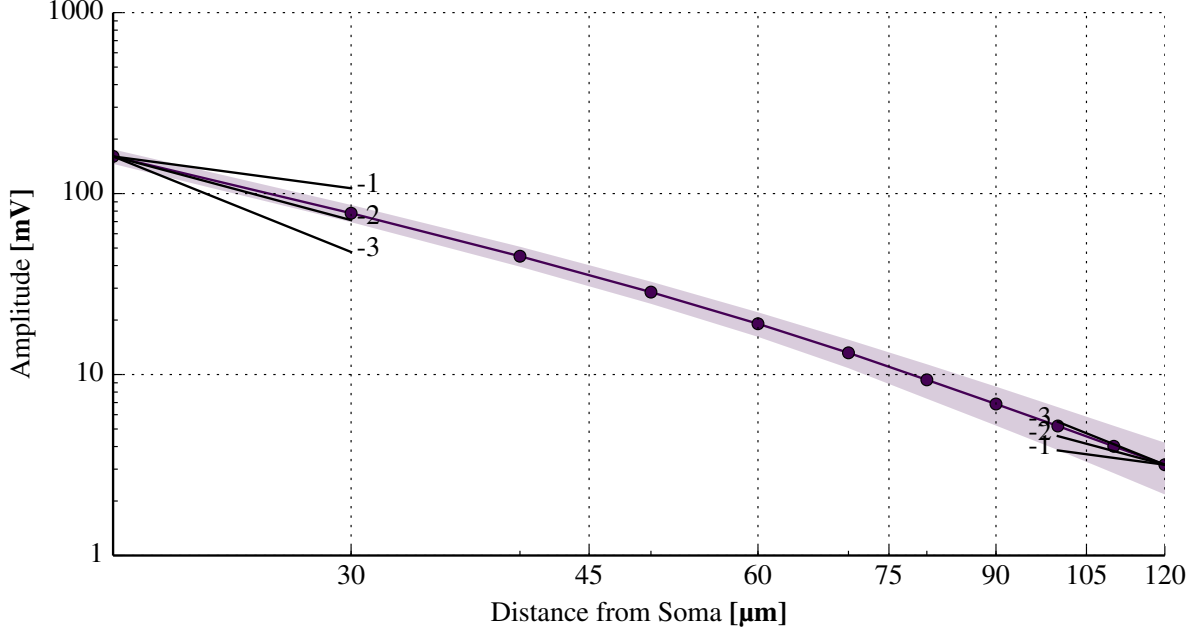


Figure 4.7: Spike amplitude over distance. Mean \pm 1 std. The power law decays $1/r$, $1/r^2$ and $1/r^3$ are shown at the leftmost and rightmost data points.

4.2 Blue Brain Model Simulations

The number of previous simulations of extracellular action potentials are few. The publicly available models from the Blue Brain (section 3.5) include neuron models with full reconstruction of the morphology. The neuron models are ment to cover the whole diversity of neuronal types encountered in the mouse somatosensory cortex. This is one of the first simulations where the extracellular action potentials of a large number of different neuronal types are being compared.

Spike width and amplitude are known to be markers for pyramidal neurons and interneurons. **Models:** Each simulation uses all available models in the L5 area. The pyramidal models consisted of models from 4 me-types with the morphologies TTPC1, TTPC2, STPC, and UTPC and the same e-type. The interneuron models consisted of the remaining 48 me-types. Each me-type had 5 models which in total summed to 20 pyramidal models and 240 interneuron models.

Each of the models a me-type were implied to have slightly different morphological shape and/or firing pattern. The degree of difference is not made clear in the documentation.

All neuron models were rotated using PCA before simulations were instigated (section 3.4).

In all simulations the extracellular conductivity was set to $\sigma = 0.3 \Omega \text{m}$ based upon data from experimental measurements.

Spike Generation:

Electrode placement: In most experiments when electrodes are placed in the brain the distance from the electrode to the neurons are usually unknown. The electrodes positions are usually adjusted until they pick up a signal from nearby neurons. To simulate this type of positioning of electrodes, the electrodes in the simulations were placed at random location around the soma.

The maximum distance an electrode can pick up the signal from neurons highly depends on the quality of the electrode used, but by today's standards the distance can usually be no longer than 100 μm . 1000 electrodes were placed around each soma within a distance of 60 μm . This max distance were chosen because even the models with the strongest extracellular amplitude were no higher than 50 μV at a distance of 60 μm . As the electrodes were randomly placed in euclidian space the number of electrodes per distance r increases as a function of r^2 . Electrodes closer than 15 μm have been ignored since not all models had any electrodes within this distance. The electrodes were placed and measured using the SphereRand (section 3.6.3) simulation class.

4.2.1 Choosing the Optimal Width Definition

Many different definitions of spike width has been used to differentiate neurons and it is not clear which spike definitions are better suited for classification. Of the most common definitions are peak-to-peak spike width and spike width measured at half amplitude (Bean (2007), fig. 4.8). Here models from the Human Brain Project has been used to question if some spike width definition prove better than others for classification.

Some investigation has previously gone into which features of the action potential are best suited for classifying neurons. Barthó et al. (2004) evaluated several spike features and concluded that the spike duration most reliably gave the best separation between pyramidal neurons and interneurons. Moreover they suggested that the peak-to-peak width definition of the unfiltered trace reliably gave the better bimodal distributions than the half-amplitude width. Their experiments were carried out in the somatosensory cortex and pre-frontal cortex of both anesthesiased and drug-free mice.

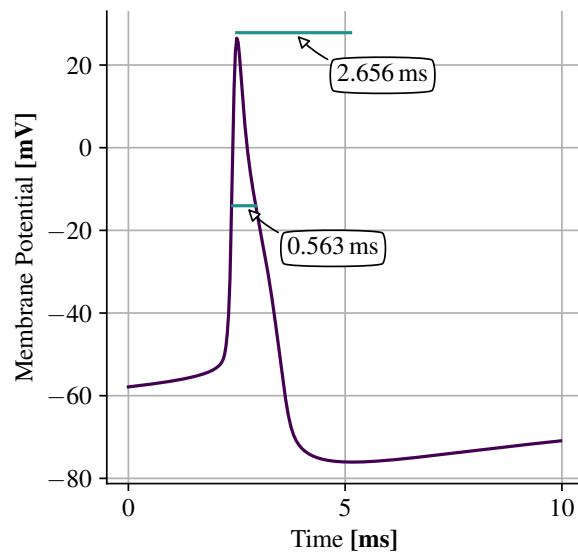


Figure 4.8: Two commonly used spike width definitions, the peak-to-peak spike width (2.656 ms) and the width at half amplitude (0.563 ms), respectively referred to as Type I and Type II in the programs. Measured from the soma from a simulation of a nested basket cell (model L5_NBC_L5_NBC_cNAC187_1).

Width Distribution: A good width definition is recognized by having a better separation between inhibitory and excitatory neurons. The extracellular spike width was recorded from each of the electrodes and binned by according to the spike width. The resulting histogram was then used for the basis of measuring the separation between neuron models (fig. 4.9).

The histograms represent a probability distribution of measuring a certain spike width given a specific neuron model.

Little overlap of the neurons models signify a good ability to separate the models into two classes. It is useful to have a metric to measure the separation between models. A proper distance metric for histogram data is already an important component for some machine learning

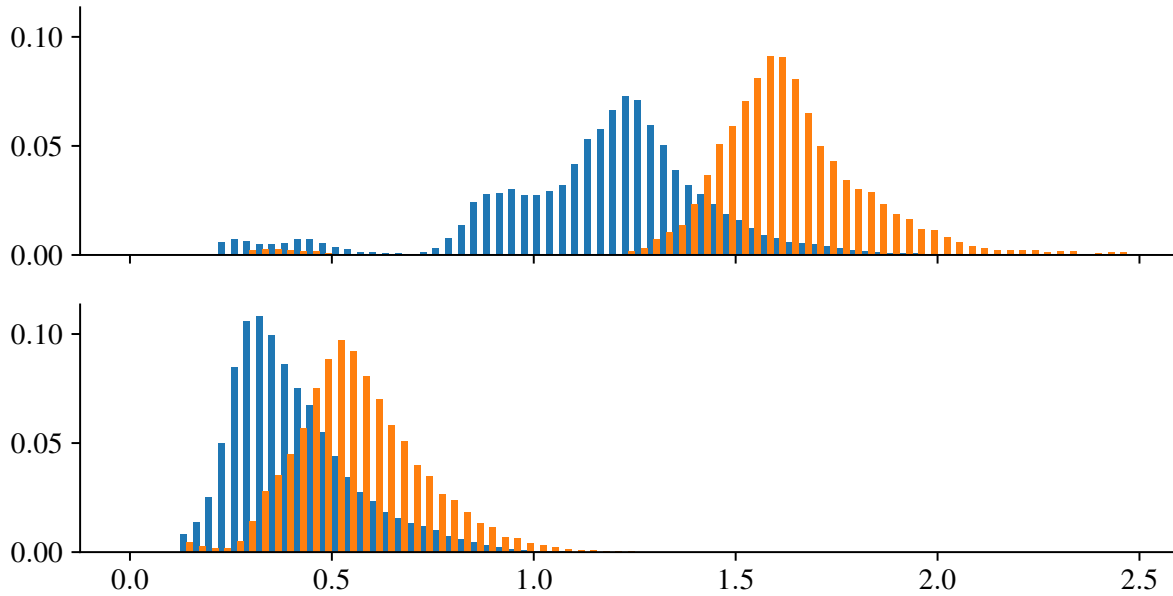


Figure 4.9: Spike widths of all L5 interneurons (blue) and pyramidal models (orange). Top histograms show peak-to-peak spike width; bottom show width at half amplitude.

tasks. This kind of binary discrimination task has been researched a lot.

Though the classification this data is better suited for a machine learning algorithm it is still useful to have a number on the separation between the neuron models. A common measure of the performance of a binary classifier is ROC curves. The area under curve of the ROC, often called the AUC, has been used as a measure of the accuracy of the classifier. The AUC of the MODEL TPPCP and LCLC was XX for the peak-to-peak definition and XX for the half-amplitude definition. In this case the peak-to-peak definition serves as a better classification criteria than half-amplitude.

Width by Distance from Soma: To make the measurements clearer neuron models of the same morphological type have been binned together and then compared to the other morphological classes.

The two spike widths were recorded and binned according to their distance from soma. The results of the simulations can be seen in [fig. 4.11](#). First it is important to note that during single unit recordings the distance to soma is usually unknown. It is still useful to know the dependence to the distance to soma. For classification purposes, if the distance to the soma is unknown it would be good if the width is constant. But most importantly that the

For both definitions the spike width of interneurons are smaller than the width of pyramidal neurons. These findings are in line with previously established research. With the Type I definition the separation between the two classes are greater in both absolute and relative value for all distances from soma. The separation between the mean of pyramidal and interneurons for Type I were 0.40 ms at 30 μm and 0.60 ms at 100 μm . For Type II the separation was 0.15 ms at 30 μm and 0.35 ms at 100 μm . These results suggest that using a type I definition of the spike width increases the chance of correctly classifying the neuron class.

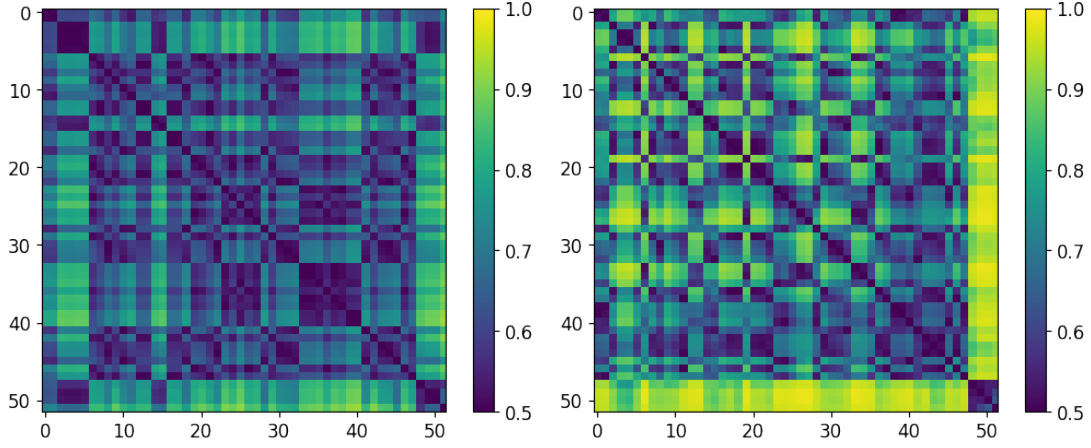


Figure 4.10: Comparisons between each group of models using ROCAUC of the width histograms. Left matrix is the half amplitude width definition; right matrix is the peak-to-peak amplitude definition. Pyramidal models can be seen bottom right corner. Higher values indicate the models can be distinguished from one another using a threshold as classification criteria. The peak-to-peak matrix indicate that all pyramidal models can be from interneurons.

In this group many of the classes represent only a very small portion of the number of neurons in L5. The findings from [Markram et al. \(2015\)](#) suggest that overall the ratio between excitatory and inhibitory neurons is around $87\% \pm 1\%$. Of these, 50% were classified as basket cells (LBC and NBC). The interneurons from L5 were separated into 9 m-types (morphological) and 10 e-types (electrophysiological) which gave a total number of 48 unique models. As such some small classes of interneurons are overrepresented in the grouped called "All Inter."

Variance: To evaluate the precision of the two width definitions it is not very useful to compare the raw variance because the mean values are different. An example is the σ at $50\mu\text{m}$ for the group "All Inter" from [fig. 4.11](#). For Type I $\sigma = 0.25\text{ ms}$ and $\mu = 1.1\text{ ms}$, while for Type II $\sigma = 0.15\text{ ms}$ and $\mu = 0.3\text{ ms}$. The variance is lower for Type II but is also almost 50% of the mean value. The variance from Type I is higher, but is only about 25% of the mean value, which makes Type I more accurate than Type II.

The coefficient of variation, c_v , is the relative variance compared to the mean.

$$c_v = \frac{\sigma}{\mu} \quad (4.1)$$

Because the variance is of similar magnitude for both width definitions, the overall greater mean of the Type I definition results in a lesser c_v at all distances, for all groups except LBC ([fig. 4.12](#)). To minimize errors when classifying neurons based on width it is best to minimize the overlap between the two definitions. Because the separation is higher and c_v is lower with Type I, this definition is better suited for classification.

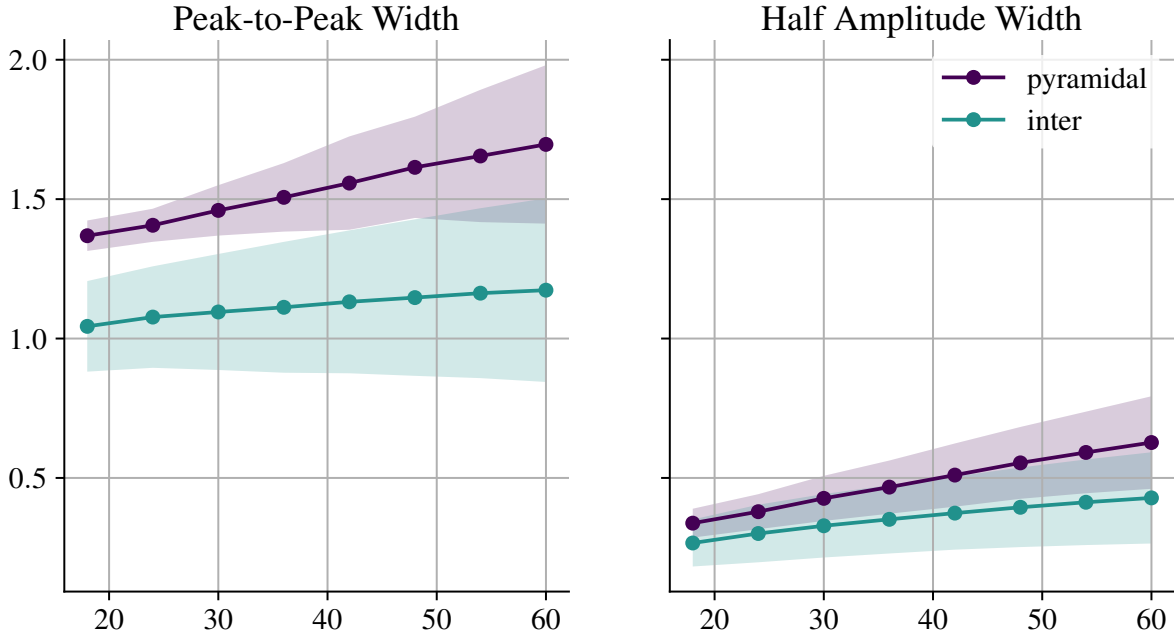


Figure 4.11: Spike widths of all L5 interneuron (top left) and pyramidal models (bottom left). Bar width equals half a simulation timestep; bin size is one simulation timestep.

4.2.2 Choosing the Optimal Amplitude Definition

The two amplitude definitions investigated are the amplitude from baseline (Type I) and the peak-to-peak amplitude definition (Type II). The simulations were ran using the same neurons and simulations as the previous section.

Figure 4.13 shows the amplitude over distance from soma. Though there is a clear separation between pyramidal neurons and interneurons at a given distance, the distance is usually unknown during experiments. The resulting histogram when ignoring distance does not show a clear bimodal distribution and is not suited as a classification parameter alone. In addition the number of electrodes increase with distance from soma where the overlap between the two functions area greater.

There seems not to be a clear distinction of which amplitude definition is better. Using amplitude alone neither is well suited as a classification parameter. As with the width definition we can calculate the coefficient of variation. The coefficient of variation is lower for the peak-to-peak width definition. This can be attributed to that the variance for both definitions are similar while the mean value of peak-to-peak amplitude is always higher.

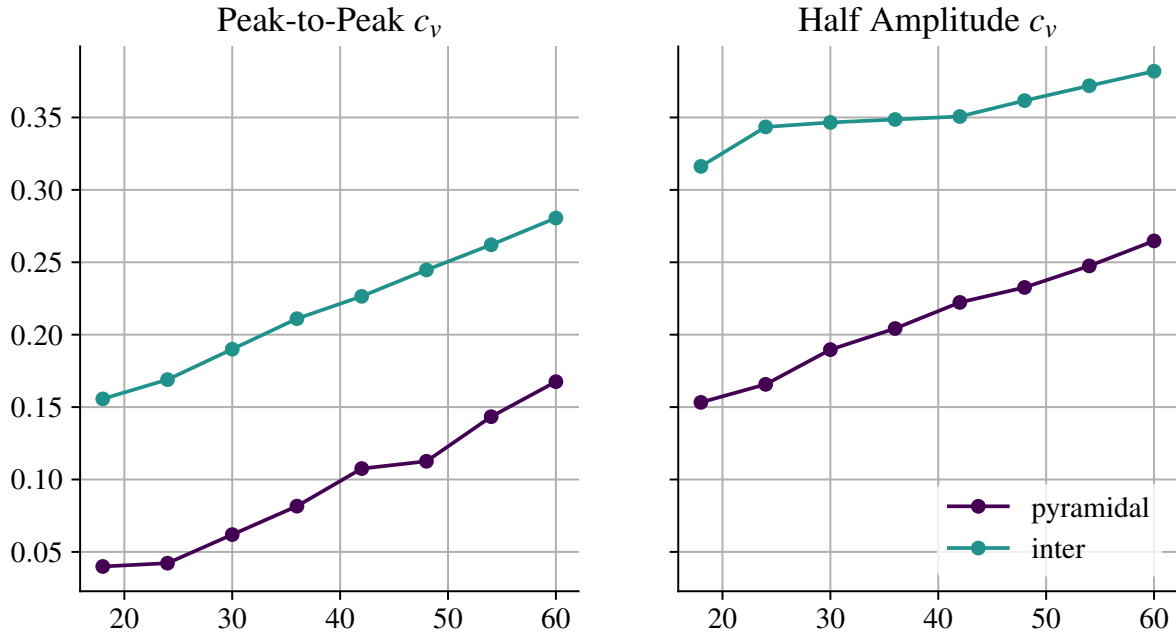


Figure 4.12: Nothing.

4.2.3 Combining Spike Width and Amplitude

As long spike widths from interneurons accompany low amplitudes and short spike widths from pyramidal neurons accompany high amplitudes it is reasonable to conclude that the amplitude could be used as an addition parameter for classification. From this point on the peak-to-peak width and amplitude definitions will be used.

The spike width and amplitude can be combined into 2d histograms as seen in the right column of figure fig. 4.14. The left column shows the histogram only based on spike width. The histograms are made from the spike width and amplitude data from all pyramidal (20) and interneuron models(250) from L5.

When combining spike amplitude and spike width it is no longer possible to apply the AUC similarity metric as was done in [Choosing the Optimal Width Definition](#) (section 4.2.1). To compare pyramidal neurons against interneurons the histograms were compared using a similarity metric defined as the histogram intersection divided by the union [Histogram Similarity Measure](#) (section 3.3). This metric can be interpreted as the overlap between the two histograms and is a valid metric for both 1d and 2d histograms.

A considerable difference was seen when comparing the overlap between the histograms. When only using spike width the overlap between interneurons and pyramidal neurons was 12.15%. In the case of spike width and amplitude the overlap was 5.10%. This suggests that using spike amplitude as an additional parameter for classification will give a more accurate result.

4.2.4 Subclasses

Pyramidal Neurons: The spike width and amp. 2d histogram of the pyramidal models has a

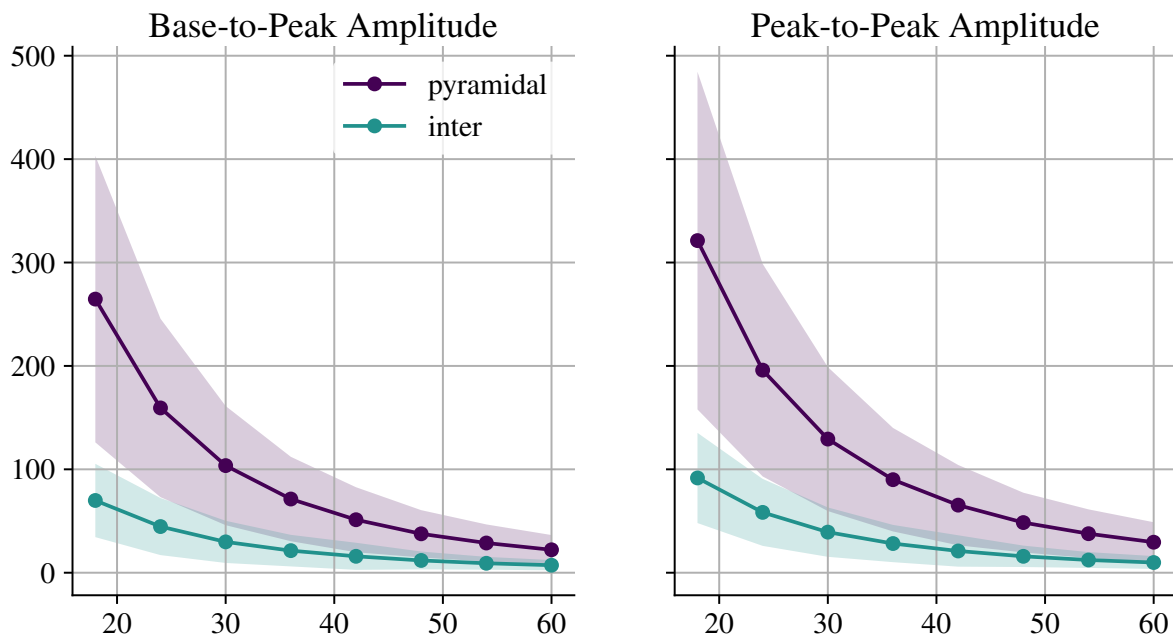


Figure 4.13: Nothing.

multimodal distribution that could suggest this group could be split into subclasses (fig. 4.14). This could be a result of a low diversity among the pyramidal models as the pyramidal data is based on 20 models versus 240 interneuron models. Though there is a much higher number of interneuron models, the number of models were based on the diversity of neurons encountered in the mouse somatosensory cortex. If the diversity in the pyramidal models correctly represent the diversity in the mouse brain it will be possible to classify some subclasses of pyramidal neurons based only on spike width and amplitude.

Figure 4.15 shows the histograms of the different classes of pyramidal neurons. where each class has 5 models. Each of these classes are a me-type but also represents the morphological class, the m-type, as the pyramidal neurons only have one e-type. The e-type of signifies a similar firing pattern based on features such as XXX. Since the firing patterns are similar the difference of the histograms show that the morphology has a big impact on the extracellular spikes. Each pyramidal models tends to have a "hockey stick" shaped distribution.

Figure 4.15 also shows the overlap between each of the classes. The two groups TTPC1 and TTPC2 has a high overlap of XX% and as such they cannot be distinguished from another. The group UTPC has little overlap with both TTPC1 and TTPC2, but overlaps STPC with XX%.

Interneurons: There is no clear multimodal distribution in the interneuron group but it might still be possible to assign models into subclasses.

4.2.5 Filtering effects

As filtering is a common manipulation of the signal to remove noise it is interesting to see if the same separation between interneurons and pyramidal neurons hold when the data is filtered. Figure 4.16 shows the same as fig. 4.14 but with the signals filtered with a bandpass butterworth filter between 300 Hz and 6.7 kHz. These values were chosen as they are reported as common

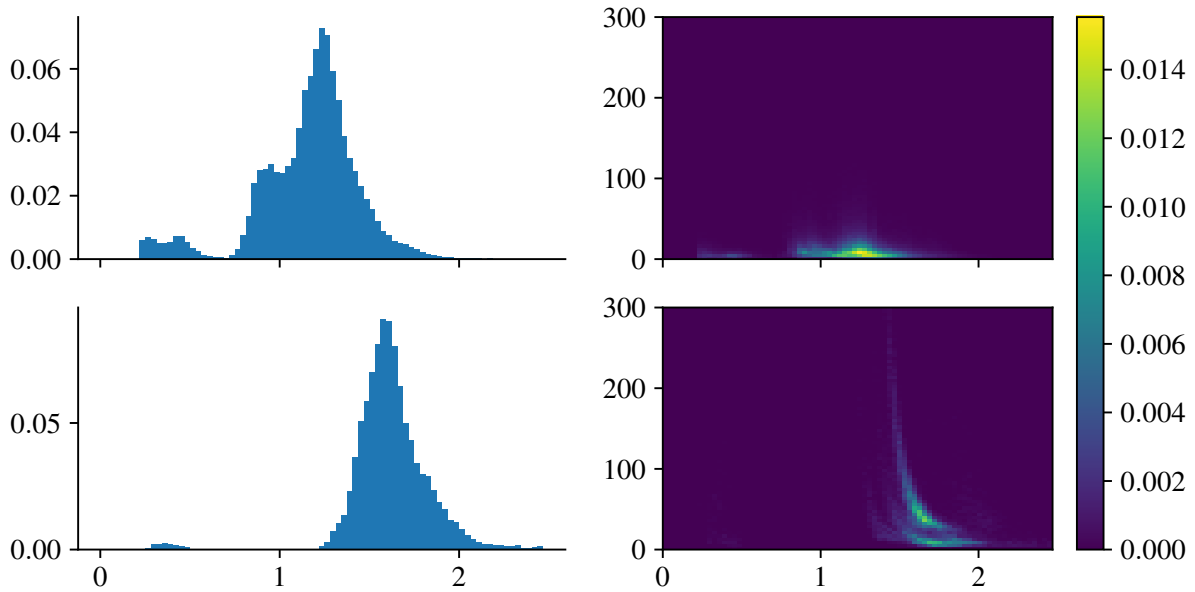


Figure 4.14: Spike width and amplitude histograms. Right column shows the combined histogram of spike amplitude and width; left column shows the distribution of only spike width. The overlap of the distributions are greater when not considering the amplitude. The overlap of the distributions for spike width alone is 12.15%. The overlap for the combined distribution of amplitude and width is 5.10%. Data basen on 240 interneuron models and 20 pyramidal models.

values for bandpassfiltering.

Though the histograms have changed drastically, the distance metric still shows that they the models can be seperated from each other by about value.

4.2.6 Comparing Results

We wanted to compare the spike widths and and amplitude found in this project with spike data from other sources. The sources used where some chosen articles, data from the bio lab and online sources.

The human Brain Project has already compared their models to multiple sources where they have a list of sources the models either agrees, disagrees or are not compatable with. The released models from HBP have no free variables as they have already been fitted to experimental data. The free parameters when doing our simulations are the extracellular conductivity constant and options to LFPy, such as representing the soma as a current sphere or as a cylindrical compartment when calculating the extracellular potential.

The page Neuroelectro has a collection of spike data from over 413 published articles. It is immediatly clear that there is a big variance in spike width data.

Bartho 2004, spike widths = 0.43 ± 0.27 ms than that of the putative pyramidal cells 0.86 ± 0.17 ms.

To further compare results our models and simulations were used to replicate some results from the paper [Anastassiou et al. \(2015\)](#). The paper was chosen because the focus of the ar-

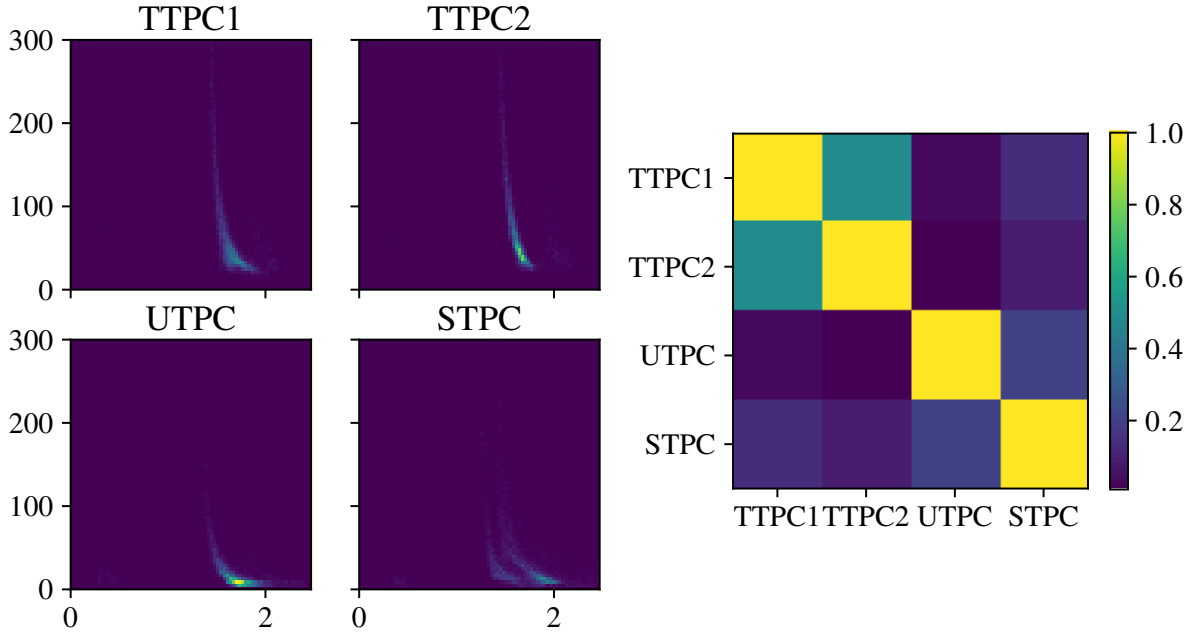


Figure 4.15: Notin.

ticle was comparing extracellular measurements to internal measurements and the brain area investigated was the somatosensory cortex.

They measured the extracellular and intracellular action potential and looked at how the shape changes as the firing rate of the neuron increases. It has been reported that the spike width of neurons increase as the firing rate increases.

The article also gives an estimate of the extracellular conductivity which was estimated by fitting the spike amplitude data to the function of the potential of a point source. $V_e = \frac{I}{\sigma} \frac{1}{4\pi r}$. The values given for the conductivity σ in L5 was $(0.41 \pm 0.24) \Omega^{-1} \text{m}^{-1}$. The high uncertainty was attributed to the estimation of the membrane capacity C .

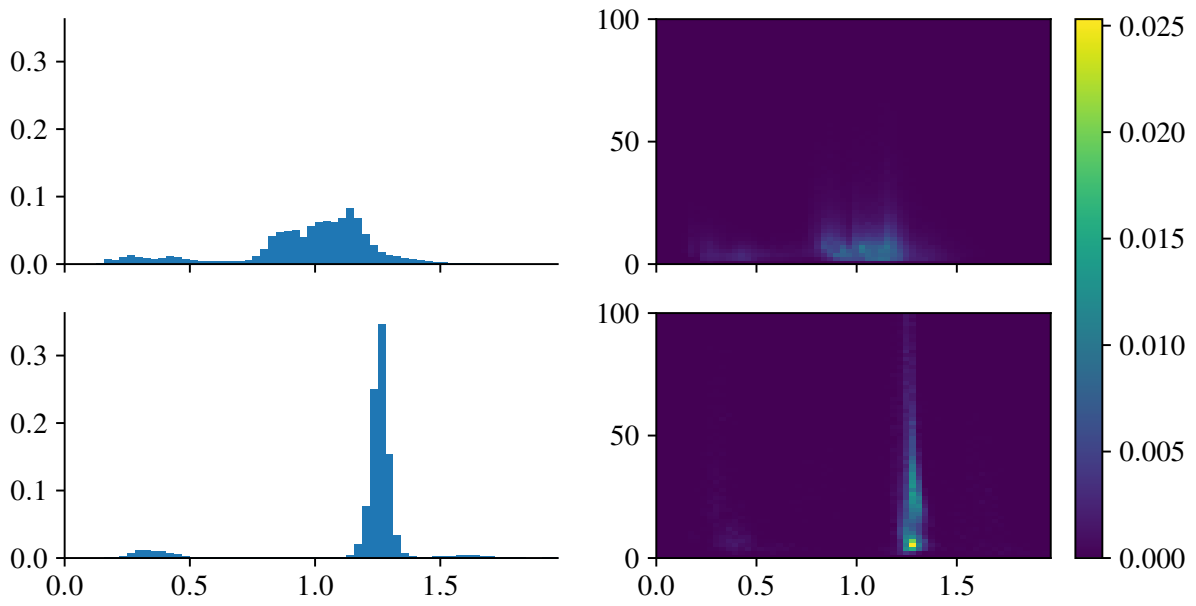


Figure 4.16: Notin.

5 | Discussion

Spike Width and Spike Amplitude: It has been seen that of the spike width definitions investigated here, one type of spike width definition is overall better suited to classify this set of neurons. This has also been seen in the literature. A similar investigation was done using the spike amplitude and of the definitions investigated here the peak-to-peak amplitude gave the best separation between interneuron and pyramidal neurons.

Classification: It has been previously shown that using only spike width as a way to classify neurons is not the best. Several papers have stated that other methods can be used to give a clearer distinction, such as considering the interspike interval. Also one group looked at the spike width from axons which gave a short duration.

Using a simple measure of the similarity between populations neuron models it can be clearly stated that interneurons can be separated from pyramidal neurons. Excitatory interneurons cannot be clearly distinguished from the rest of the interneurons. Using machine learning algorithms it might be possible to divide these into even small groups, how can I show this? Neurons could probably be separated into smaller groups based on spike width and spike amplitude.

LFPyUtil: LFPyUtil is a useful tool that can be used to easily gather new data when new models arrive. As long as a model has the mechanics defined with NEURON and has a morphology the same simulations and data as seen here can be ran and extracted.

The models did now show the expected variance with firing frequency.

Comparisons with other data: several articles were investigated to compare current data with. There is a large variance in the literature of spike widths and amplitude. All in all the data fall within the variance of the investigated articles. The number range between this and that.

Sources of variation:

A | Appendix

```
1 import LFPy
2 import LFPy_util
3 import os
4 import numpy as np
5 import neuron
6 from glob import glob
7
8 # Location of the models.
9 DIR_FILE = os.path.dirname(os.path.realpath(__file__))
10 DIR_MODELS = os.path.join(DIR_FILE, 'res/')
11
12 def get_cell(neuron_name):
13     """
14     Load a spesific model based on a string and return a LFPy Cell object.
15     :param string neuron_name:
16         String to identify the neuron model that will be loaded.
17     :return:
18         Cell Object from LFPy.
19     """
20     original_cwd = os.getcwd()
21     neuron.h.load_file('stdrun.hoc')
22     neuron.h.load_file('import3d.hoc')
23
24     # Use the neuron name to find the desired model.
25     dir_nrn_model = os.path.join(DIR_MODELS, neuron_name)
26
27     # Load mod files of the neuron.
28     mechanism_mod_dir = os.path.join(dir_nrn_model, 'mechanisms')
29     LFPy_util.other.nrnivmodl(mechanism_mod_dir)
30
31     # The following .hoc files are spesific for the blue brain models.
32     os.chdir(dir_nrn_model)
33     #get the template name
34     tmp_file = file("template.hoc", 'r')
35     templatename = get_templatename(tmp_file)
36     tmp_file.close()
37     #get biophys template name
38     tmp_file = file("biophysics.hoc", 'r')
39     biophysics = get_templatename(tmp_file)
40     tmp_file.close()
41     #get morphology template name
42     tmp_file = file("morphology.hoc", 'r')
43     morphology = get_templatename(tmp_file)
44     tmp_file.close()
45     #get synapses template name
46     tmp_file = file(os.path.join("synapses", "synapses.hoc"), 'r')
47     synapses = get_templatename(tmp_file)
48     tmp_file.close()
49     neuron.h.load_file('constants.hoc')
50
51     if not hasattr(neuron.h, templatename):
52         # Load main cell template
53         neuron.h.load_file(1, "template.hoc")
54     if not hasattr(neuron.h, morphology):
55         # Load morphology
56         neuron.h.load_file(1, "morphology.hoc")
57     if not hasattr(neuron.h, biophysics):
58         # Load biophysics
59         neuron.h.load_file(1, "biophysics.hoc")
60     if not hasattr(neuron.h, synapses):
61         # load synapses
62         neuron.h.load_file(1, os.path.join('synapses', 'synapses.hoc'))
63
64     for morphologyfile in glob('morphology/*'):
65         # Instantiate the cell(s) using LFPy
66         cell = LFPy.TemplateCell(
67             morphology=morphologyfile,
68             templatefile=os.path.join(neuron_name, 'template.hoc'),
69             templatename=templatename,
70             templateargs=0,
71             tstartms=0,
72             tstopms=300.,
73             pt3d=True,
74             timeres_NEURON=2 ** -5, 46
75             timeres_python=2 ** -5,
76             passive=False,
77             v_init=-70,
78         )
79     # Reset back to the previous working directory.
```


Bibliography

- Anastassiou, Costas A. et al. (2015). “Cell type- and activity-dependent extracellular correlates of intracellular spiking.” en. In: *Journal of Neurophysiology* 114.1, pp. 608–623. ISSN: 0022-3077, 1522-1598. (Visited on 05/04/2016).
- Barthó, Peter et al. (2004). “Characterization of neocortical principal cells and interneurons by network interactions and extracellular features.” eng. In: *Journal of Neurophysiology* 92.1, pp. 600–608. ISSN: 0022-3077.
- Bean, Bruce P. (2007). “The action potential in mammalian central neurons.” en. In: *Nature Reviews Neuroscience* 8.6, pp. 451–465. ISSN: 1471-003X. (Visited on 04/25/2016).
- Connor, J. A. & C. F. Stevens (1971). “Prediction of repetitive firing behaviour from voltage clamp data on an isolated neurone soma.” In: *The Journal of Physiology* 213.1, pp. 31–53.
- Connor, J. A., D. Walter, & R. McKown (1977). “Neural repetitive firing: modifications of the Hodgkin-Huxley axon suggested by experimental results from crustacean axons.” In: *Biophysical Journal* 18.1, pp. 81–102. ISSN: 0006-3495. (Visited on 11/13/2015).
- Dayan, Peter & Laurence F. Abbott (2001). *Theoretical neuroscience*. Vol. 806. Cambridge, MA: MIT Press. (Visited on 11/12/2015).
- Hämäläinen, Matti et al. (1993). “Magnetoencephalography- theory, instrumentation, and applications to noninvasive studies of the working human brain.” In: *Reviews of modern Physics* 65.2, p. 413.
- Hodgkin, Alan L. & Andrew F. Huxley (1952). “A quantitative description of membrane current and its application to conduction and excitation in nerve.” In: *The Journal of physiology* 117.4, pp. 500–544.
- Lindén, Henrik et al. (2013). “LFPy: a tool for biophysical simulation of extracellular potentials generated by detailed model neurons.” In: *Frontiers in neuroinformatics* 7.
- Mainen, Zachary F. & Terrence J. Sejnowski (1996). “Influence of dendritic structure on firing pattern in model neocortical neurons.” In: *Nature* 382.6589, pp. 363–366. (Visited on 11/13/2015).
- Markram, Henry et al. (2015). “Reconstruction and simulation of neocortical microcircuitry.” In: *Cell* 163.2, pp. 456–492.
- Mountcastle, Vernon B. et al. (1969). “Cortical neuronal mechanisms in flutter-vibration studied in unanesthetized monkeys: Neuronal periodicity and frequency discrimination.” In: *Journal of neurophysiology*.
- Pettersen, Klas H. & Gaute T. Einevoll (2008). “Amplitude variability and extracellular low-pass filtering of neuronal spikes.” In: *Biophysical journal* 94.3, pp. 784–802.

- Ramaswamy, Srikanth et al. (2015). “The neocortical microcircuit collaboration portal: a resource for rat somatosensory cortex.” In: *Frontiers in Neural Circuits*, p. 44. (Visited on 08/01/2016).
- Sterratt, David et al. (2011). *Principles of computational modelling in neuroscience*.